Acta of Bioengineering and Biomechanics
Vol. 22, No. 4, 2020

Original paper
DOI: 10.37190/ABB-01664-2020-04

Osteointegration technology in long bone defect reconstruction: experimental study

ARNOLD POPKOV, NATALIA KONONOVICH, ELENA GORBACH, DMITRY POPKOV*

Ilizarov National Medical Research Center for Traumatology and Orthopedics, Kurgan, Russia.

Purpose: The purpose of this experimental study was to evaluate the osteointegration of a bioactive 3D-cylindrical titanium-alloy implant (bone-graft substitute) for tibial shaft defect reconstruction. *Methods*: An experimental study was done in 7 mongrel dogs. Tibial shaft defect was repaired using an original titanium-alloy (Ti6Al4V) cellular cylindrical implant. with a bioactive layer of hydroxyapatite by anode microarc oxidation. Histological study (hematoxylin-eosin stain and immunohistological reaction using ostepontin polyclonal antibodies) and scanning electron microscopy (electron probe X-ray microanalysis for calcium and phosphorus saturation in the tissue matrix) were applied to assess bone tissue regeneration. *Results*: Experimental study revealed osteoconduction starting from the endosteum of bone fragments adjacent to the bone defect and developed to the central part of the implant. In 4 weeks, graft osteointegration was achieved in all animals. Implant cells were filled with spongy bone tissue and the graft external surface was covered with a connective tissue structures similar to the periosteum ones. *Conclusions*: Cellular titanium bone-graft substitute with bioactive coatings placed into bone defect stimulates reparative osteogenesis and graft osteointegration.

Key words: *bone-graft substitute, hydroxyapatite coating, osteointegration*

1. Introduction

Materials for large bone defect reconstruction have to fulfill large spectrum of requirements including high resistance to mechanical load. Metallic biomaterials such as titanium in the form of porous implants [1] have high mechanical load capacities and could correspond to these requirements. On the other hand, the ideal bone graft material for large diaphyseal defect reconstruction is a scaffold promoting new bone tissue formation and remodeling, and acting as a pathway for bone regeneration [2]. Not degradable materials provide only a replacement of the anatomical function rather than bone regeneration. High stiffness of metallic biomaterials results in a stress-shielding effect leading to loss of additional bone tissue surrounding implants [3]. The materials with an intrinsic microporosity and macropores are recommended for enhanced new bone formation [4], but negative effect of porosity on mechanical capacity of implants is well-known and highly porous bone graft substitutes are unsuitable for mechanically-loaded long bone reconstruction [5].

Biomaterials used in bone defect repairing should provide osteoinductivity. But it is still limited compared to the one of rhBMP-2 [6]. The recombinant human bone morphogenetic protein-2 has high bone regeneration capability, stimulates the mesenchymal stem cells to differentiate, transforms preosteoblasts into osteoblasts, and acts as a trigger for migration of osteoblasts [7], but the release of rh-BMP-2 causes numerous complications such as heterotopic ossifications, osteolysis and cancer [7], [9].

Coating of surfaces with hydroxyapatite (HA) improves bioactivity and osteointegration of metallic

* Corresponding author: Dmitry Popkov, Clinic of Neuroorthopaedics and Systemic diseases, Ilizarov National Medical Research Center for Traumatology and Orthopedics, M. Ulyanova str. 6, 640014, Kurgan, Russia. E-mail: dpopkov@mail.ru

Received: May 27th, 2020
Accepted for publication: September 16th, 2020

implants [10]. It was shown only for implants with bioactive surfaces that primary implant stability is favored by HA-coating which results in an improved contact between bone and implant [11]. The studies demonstrated a sufficient osteointegration of HA-coated hip implants [10]. HA is thought to be an osteoconductive material that shows osseoinductive capacity with ectopic bone formation [12], [13]. The osteoinductive layer of HA on the implant can be achieved using microarc oxidation in an electrolyte containing calcium and phosphate or by composite coating including fluorocarbon plastic (copolymer of tetrafluoroethylene and vinylidenfluoride) filled with finely dispersed hydroxyapatite [12], [13].

On the other hand, a promising approach in limb reconstructive surgery regardless of osteoinductive features of implants is presented by of customized endoprostheses. This approach can reduce limb sparing surgery time and associated risk of implant failure [14].

Currently, there are no morphological and histological studies demonstrating osteointegration of implants with both intrinsic microporosity and internal osteoinductive layer in experimental, mechanically-loaded long bone defect reconstruction. Thereby, the purpose of this experimental study was to assess the osteointegration of the 3D scaffold porous calcium phosphate-coated cylindrical titanium implant placed into bone defect of mechanically-loaded long bone.

2. Materials and methods

Seven scaffold porous calcium phosphate-coated cylindrical titanium (Ti6Al 4V) implant was used in this study of bone defect reconstruction (Fig. 1a). The internal surface of the cylinder was divided into cells of 1.5 mm in diameter and 0.5 mm in wall thickness. The cells and pores in cylindrical external walls were of 300–500 μm in diameter to enhance bone formation and the invasion of capillaries from the part of periosteal structures and adjacent bone fragments. Rims on the implant plane surface had orifices for screw fixation to bone proximal and distal fragments and small pores (100–300 μm) to provide bone and vascular ingrowth from the periosteal part favorable for implant osteointegration. The implants were made and customized depending on the diameter and shape of transversal section image of middle part of tibial shaft reconstructed from the dog's CT scans. Their transverse dimension varied from 13 to 18 mm. The length of 3D scaffold part corresponded to 15% of operated tibia varying from 27 to 31 mm. The implant external and internal, intracellular surfaces had a bioactive layer using the technology of anode microarc oxidation (MAO) in an electrolyte containing calcium and phosphate compounds [13], [15].

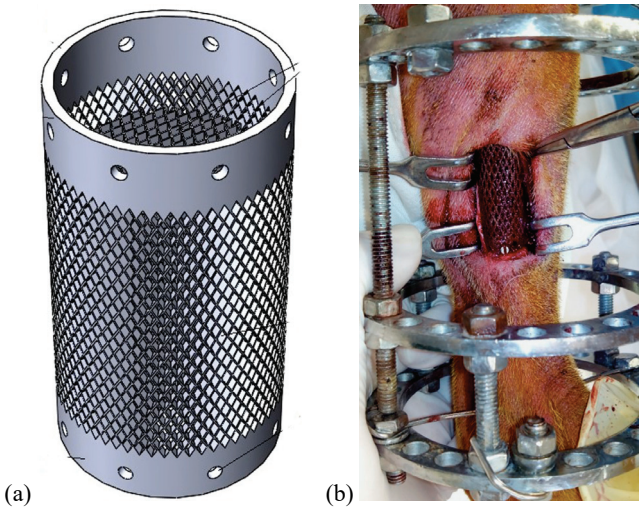

Fig. 1. Tibial shaft defect reconstruction:
(a) schematic of cylindrical implant,
(b) cylindrical bone-graft substitute placed into the bone defect, Ilizarov frame application

The experiment was conducted on 7 dogs aged 1–3 years. Their mean body mass was 20 ± 2.9 kg. The experimental surgeries were performed by one surgical team. All the surgical interventions were performed under general anesthesia with the sodium thiopental 5% solution (10–15 mg/kg). Through anterior approach, a total defect of 15% segment length was done by subperiosteal resection in the middle third of tibial shaft (Fig. 1b). Then, customized cylindrical implant was placed into the space between tibial fragments and fixed with screws. A one third of circumference of anterior periosteum over the implant was resected as well. When the wound sutured, Ilizarov frame was applied. The fixators comprised two distal and two proximal rings connected by three threaded rods. Three stain steel 1.5-mm wires were inserted in proximal tibial fragment and three wires of the same diameter were inserted in the distal tibial fragment. All wires were tensioned with 100 kg forces. The external frame fixation lasted for two weeks in each animal. In contrast to rigid half-pins, an external fixator with wires provided biomechanical benefit with the weight bearing on the bone regenerate during walking and does not demonstrate stiffness with negative influence on bone remodelling [16], [17]. Cefazolin was administered intramuscularly for 7 days after the surgery (0.5 g twice a day). The wounds underwent daily control.

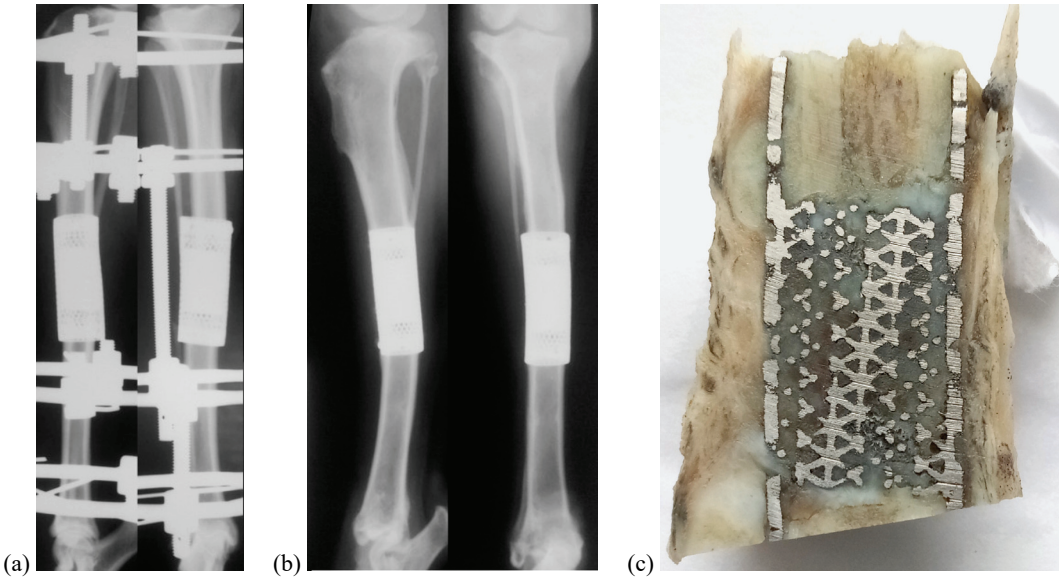

Fig. 2. Radiographic images of the tibia after the surgery, 3D scaffold placed into bone defect:
(a) Ilizarov frame application, (b) radiographic images after frame removal, in 4 weeks after surgery,
(c) – dissected bone sample with implant in 29 days after the surgery

AP and lateral X-rays were taken on the day of surgery and then every two weeks (Figs. 2a, b). Upon completion of euthanasia in 28 days after surgery, 4-cm-long full diaphyseal fragment was sawn out.

Histological sections, 20–24 mm thick, were obtained with a sledge microtome (Reichard, Germany), stained with hematoxylin and eosin and according to Van Gieson. Histological bone tissue preparations were studied with a large microscope (Carl Zeiss Opton, Germany).

Immunohistological reaction using ostepontin polyclonal antibodies as per Abcam protocol (United Kingdom) were examined with AxioScope.A1 stereomicroscope and AxioCam ICc 5, and completed with Zen blue software («Carl Zeiss MicroImaging GmbH», Germany).

Bone-implant block dried using an original technology [18] was examined using an X-ray electron probe microanalyzer (INCA-200) on the basis of JSM-840 scanning electron microscope. The content of calcium and phosphorus in the tissue matrix was determined inside the implant cells and on the implant surface.

The study results were processed using non-parametric statistics. The statistical significance between two samples was estimated with Wilcoxon *W*-criteria for independent samples.

Longitudinal samples of the bone-implant block were achieved using MECATOME T210 cutting (180 mm diameter abrasive disc, 0.5 mm depth, 2000 rotations per minute disk speed, 0.2 mm/s table translational velocity machine; PRESI, France) (Fig. 2c).

The data were analyzed using nonparametric statistics in AtteStat 10.8.8 version for Microsoft Excel. The reliability of differences was determined with the Wilcoxon *W*-test for independent samples.

The experiments were carried out in accordance with the requirements of the European Convention for the Protection of Vertebrates Used for Experimental and Other Scientific Purposes (Strasbourg, 1986), in accordance with the principles of laboratory practice (NIH Publication no.85-23, revised 1985), and were approved by the ethics board of our institution.

3. Results

The dogs were observed for 28 days after surgery until euthanasia. No changes in animals' general health or food and water consumption were observed during the study. There were no septic or neurological complications. Animals started to walk with weight-bearing on the operated limb since 2nd–3rd day post-operatively. Weight-bearing function of the experimental limb was maintained until the end of the study.

Radiological methods did not enable to show endosteal bone formation since a titanium implant is not transparent to X-rays, but limited periosteal reaction was observed over the implant ends (Fig. 2b).

All of the animals survived during the healing periods without adverse effects, such as local or general infection, inflammation, and specimen exposure at surgical sites.

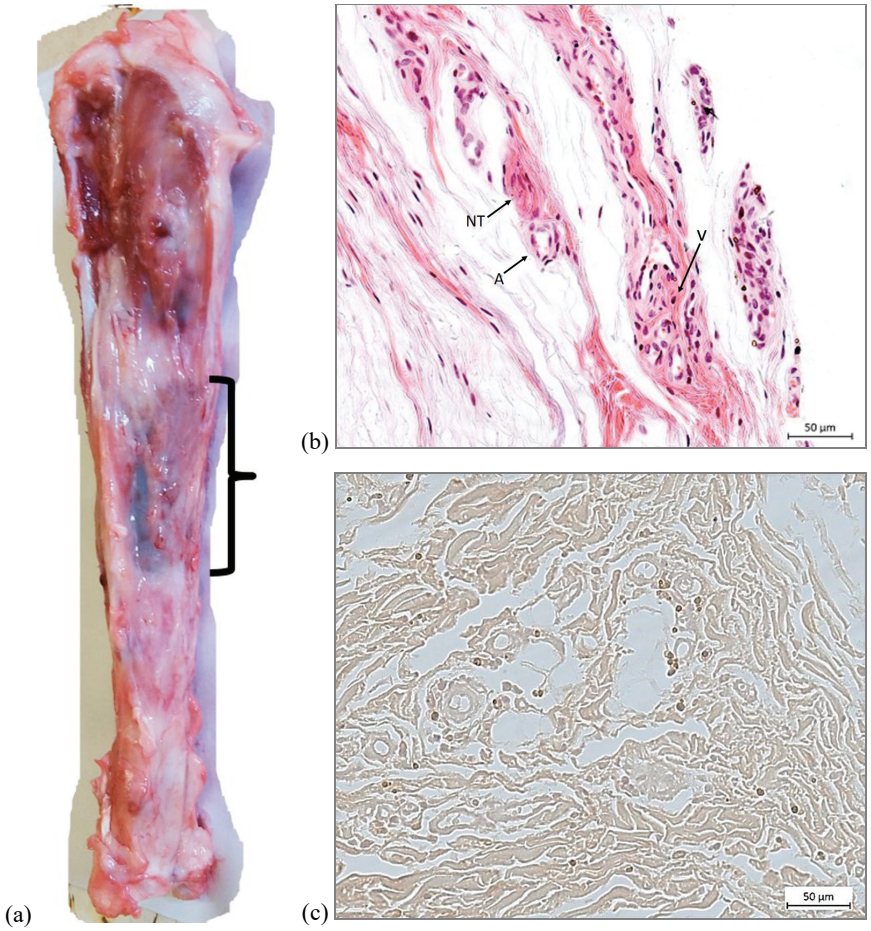

Fig. 3. Morphology 29 days after surgery: (a) tibia, soft tissues removed,
a connective tissue thin layer (similar to periosteum) covers the implant surface,
(b) histological study of the covering layer (NT – nerve trunk, A – artery, V – vein),
hematoxylin-eosin staining, 400× magnification, (c) ostopontin expression in perivascular periosteal cells
formed on the surface of the implant proximal portion
(immunohistochemical staining with osteopontin polyclonal antibodies)

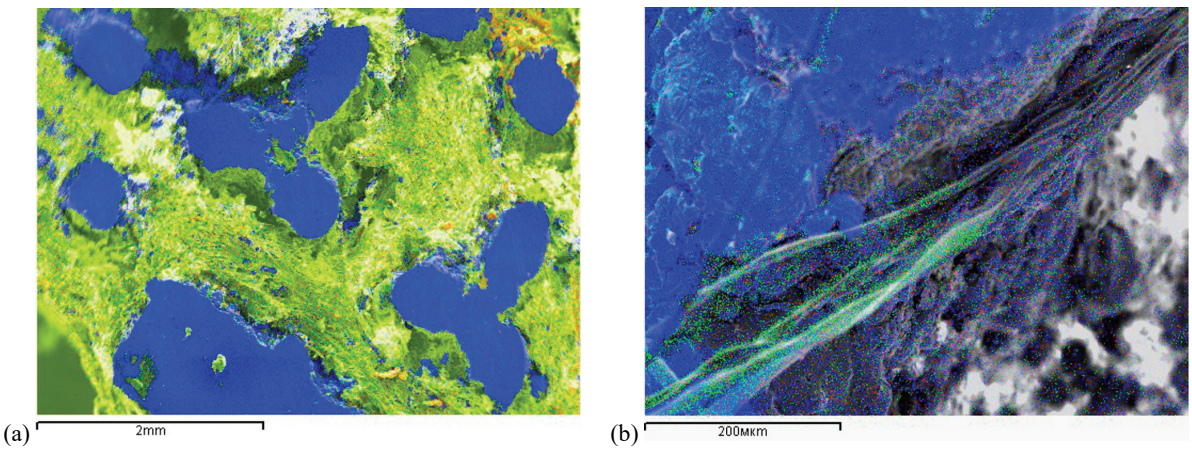

Fig. 4. The bone-implantat block structure in 29 days after the surgery
a) ingrowth of the bone tissue into the implant cells, (b) microvascular invasion into the implant cells.
Combined maps of the X-ray electronic and probe microanalysis
obtained during characteristic radiation of Ca, P, Ti. Magnification: a – 20×; b – 200×.
Blue – Ti, light-green – a mixed overlapping of Ca and P

28 days after surgery, histological study revealed alveolar connective tissue formed on the surface of the cylinder (Fig. 3a,b). Its structure was similar to the one of the periosteum. Vessels and nervous tubes were visualized. The newly formed periosteal tissue had ostopontin-expressing cells found in perivascular and adjacent areas (Fig. 3c).

The longitudinal section sample of the bone-implant block has shown that by the 28th day after the surgery, all implant cells were filled with bone substance with density similar to the one of cancellous bone (Fig. 2c) located in the medullary cavity in the proximity of the implant. Osteointegration was almost totally achieved when osseous tissue ingrowth was observed into the implant pores and cells.

The maps of X-ray electron probe microanalysis revealed bone tissue ingrowth into all implant cells (Fig. 4), however, its highest mineralization was found in the cells adjacent to the implant proximal end.

According to qualitative X-ray electron and probe microanalysis, the most mineralized bone tissue was found in proximal areas of implant. The bone tissue was less mineralized in the implant central and distal parts (Table 1).

In all assessed areas, Ca/P ratio in the tissue matrix exceeded 2. Thus, crystalline hydroxyapatite predominated in the bone matrix. No mineral component outflow (Ca and P) from the bone fragments was observed. Their content was statistically close to normal values. The applied hydroxyapatite coating induced osteogenesis over the implant surfaces. This was demonstrated by the presence of osseous tissue and was confirmed by the X-ray electron and probe analysis (Table 1).

4. Discussion

The Ilizarov method is indicated for non-unions. It ensures bone union and simultaneous lengthening and deformity correction. However, its numerous inconveniences are well-known and recognized: long time lasting external fixation (4 to 12 months, healing index over 40 days/cm), high risks of complications (pin site infection, deep infection, secondary joints stiffness) and strong psychological impact on the patient due to long duration of external fixator wearing and common complications [19].

That is why there is a large interest to apply bone substitute implants for large defects of bones. These bone graft substitutes should have sufficient load capacity for orthopedic applications [1], [20]. Unfortunately, the implant design is usually focused on fast tissue ingrowth and bone regeneration having porous structure with an intrinsic microporosity [21] and gets

Table 1. Content of Ca and P in the cellular implant tissue matrix

Bone-implant block examination area	Percent by weight [%]		
	Ca	P	Ca/P
Tissue matrix in the implant proximal cells, intermediary area	3.68 ± 0.17*	1.64 ± 0.03*	2.24 ± 0.06
Tissue matrix in the implant central cells, intermediary area	3.04 ± 0.13*	1.45 ± 0.06*	2.1 ± 0.08
Tissue matrix in the implant distal cells, intermediary area	3.65 ± 0.11*	1.66 ± 0.07*	2.2 ± 0.001
Tissue matrix in the implant proximal cells in the medullary canal zone	6.55 ± 0.24*	2.62 ± 0.11*	2.5 ± 0.02
Tissue matrix in the implant central cells in the medullary canal zone	3.2 ± 0.12*	1.52 ± 0.04*	2.1 ± 0.03
Tissue matrix in the implant distal cells in the medullary canal zone	3.20 ± 0.11*	1.28 ± 0.03*	2.5 ± 0.026
The cortex of proximal bone fragment	21.57 ± 0.8	9.71 ± 0.45	2.22 ± 0.09
The cortex of distal bone fragment	20.60 ± 0.7	8.7 ± 2.2	2.37 ± 0.02
The medullary canal of the proximal bone fragment	9.95 ± 0.37*	4.54 ± 0.21*	2.19 ± 0.02
The medullary canal of the distal bone fragment	9.84 ± 0.24*	3.9 ± 0.18*	2.52 ± 0.05
The cortex of intact tibia (normal control values)	22.02 ± 0.9	10.11 ± 0.33	2.18 ± 0.06

* – The values are significantly different from the normal values ($p < 0.05$).

unsuitable for mechanically-loaded orthopedic application [5]. In our opinion, only metallic scaffold--structured biomaterials with capacity of fast osteointegration fulfill all demanding requirement for long bone defect reconstruction.

Previous morphological studies revealed an osseoinduction effect related to hydroxyapatite coating of intramedullary implants [22]. Rough surface with pores enables microvascular and bone formation with dense trabecular structure on the implant without a connective tissue between implant and newly formed bone tissue [22], [23].

In our study, 3D titanium implant with bioactive external and internal surfaces induced the formation of continuous connections between endosteal tissue and implant surface filling in the medullary canal with cancellous bone and making the implant osteointegration complete. Formation of the osseous tissue is mainly associated with the angiogenesis that ensures cellular migration enhanced by pores in the implant.

We hypothesize that perivascular cells and mesenchymal osteoprogenitor cells activated by broken bone integrity migrate toward the implant cells. In the presence of hydroxyapatite on the surface of both the external and internal implant structures, mesenchymal osteoprogenitor cells during osteogenesis differentiate into osteoblasts providing osseous trabeculae [24], [25]. The mechanism revealed in our study was confirmed by osteopontin expression in perivascular cells, bone matrix on the surface of microvessels growing into the implant cells, osseous bone formation in the cellular structures of the bone-substitute implant. Implant covering tissue functions as a periosteum.

5. Conclusions

Experimental reconstruction of bone defects with 3D scaffold cylindrical implants ensuring osteoinduction by bioactive internal and external coating demonstrated its effectiveness. In our study, this approach provided primary stability and fast implant osteointegration without any loosening of the implants. Development of this type of customized bioactive osteosynthesis seems to be promising for long bone defect reconstruction in human.

Data availability

The data used to support the findings of this study are available from the corresponding author upon request.

Ethical approval

All applicable international, national, and/or institutional guidelines for the care and use of animals were followed.

References

[1] GEETHA M., SINGH A.K., ASOKAMANI R., GOGIA A.K., *Ti-based biomaterials, the ultimate choice for orthopaedic implants. A review*, Prag. Mater Sci., 2009, 54, 397–425.

[2] GUARINO V., CAUSA F., AMBROSIO L., *Bioactive scaffolds for bone and ligament tissue*, Expert. Rev. Med. Devices, 2007, 4, 405–418.

[3] NOYAMA Y., MIURA T., ISHIMOTO T., ITAYA T., NIINOMI M., NAKANO T., *Bone loss and reduced bone quality of the human femur after total hip arthroplasty under stress-shielding effects by titanium-based implant*, Mater. Trans., 2012, 53, 565–570.

[4] DOROZHKIN S., *Calcium Orthophosphate-Based Bioceramics*, Materials, 2013, 6, 3840–3942.

[5] ZHANG J., LIU W., SCHNITZLER V., TANCRET F., BOULER J.-M., *Calcium-phosphate cements for bone substitution: chemistry, handling and mechanical properties*, Acta Biomater., 2014, 10, 1035–1049.

[6] CHAN O., COATHUP M., NESBITT A., HO C.Y., HING K., BUCKLAND T., CAMPION C., BLUNN G., *The effects of microporosity on osteoinduction of calcium phosphate bone graft substitute materials*, Acta Biomater., 2012, 8, 2788–2794.

[7] LIU S., LIU Y., JIANG L., LI Z., LEE S., LIU C., WANG J., ZHANG J., *Recombinant human BMP-2 accelerates the migration of bone marrow mesenchymal stem cells via the CDC42/PAK1/LIMK1 pathway in vitro and in vivo*, Biomater. Sci., 2018, 7, 362–372.

[8] TANNOURY C.A., AN H.S., *Complications with the use of bone morphogenetic protein 2 (BMP-2) in spine surgery*, Spine J., 2014, 14, 552–559.

[9] STEIB J.-P., BOUCHAIB J., WALTER A., SHULLER S., CHARLES P., *Could an osteoinductor result in degeneration of a neurofibroma in NF 1?*, Eur. Spine J., 2010, 19 (Suppl. 2), S220–S225.

[10] ZWEYMULLER K.A., *Bony ongrowth on the surface of HA-coated femoral implants: an x-ray analysis*, Z. Orthop. Unfall., 2012, 150 (1), 27–31.

[11] POPKOV A.V., GORBACH E.N., KONONOVICH N.A., POPKOV D.A., TVERDOKHLEBOV S.I., SHESTERIKOV E.V., *Bioactivity and osteointegration of hydroxyapatite-coated stainless steel and titanium wires used for intramedullary osteosynthesis*, Strategies in Trauma and Limb Reconstruction, 2017, 12 (2), 107–113.

[12] BOLBASOV E.N., POPKOV D.A., KONONOVICH N.A., GORBACH E.N., KHLUSOV I.A., GOLOVKIN A.S., STANKEVICH K.S., IGNATOV V.P., BOUZNIK V.M., ANISSIMOV Y.G., TVERDOKHLEBOV S.I., POPKOV A.V., *Flexible intramedullary nails for limb lengthening: a comprehensive comparative study of three nails types*, Biomed. Mater., 2019, 4 (2), 025005.

[13] BOLBASOV E.N., POPKOV A.V., POPKOV D.A., GORBACH E.N., KHLUSOV I.A., GOLOVKIN A.S., SINEV A., BOUZNIK V.M., TVERDOKHLEBOV S.I., ANISSIMOV Y.G., *Osteoinductive composite coatings for flexible intramedullary nails*, Materials Science and Engineering C, 2017, 75, 207–220.

[14] TIMERCAN A., BRAILOVSKI V., PETIT Y., LUSSIER B., SEGUIN B., *Personalized 3D-printed endoprostheses for limb sparing in dogs: Modeling and in vitro testing*, Med. Eng. Phys., 2019, 71, 17–29.

[15] POPKOV A.V., POPKOV D.A., KONONOVICH N.A., TVERDOKHLEBOV S.I., *Cellular cylindrical bioactive implant to replace circular defects of tubular bones*, Patent No. 171823 dated 16.05.2017. Application No. 2016152351/14(083849). Priority as of 28.12.2016.

[16] GOODSHIP A.E., KENWRIGHT J., *The influence of induced micromovement upon the healing of experimental tibial fractures*, J. Bone Jt. Surg. Br. Vol., 1985 Aug., 67 (4), 650–655.

[17] MERLOZ P., MAUREL N., MARCHARD D., LAVASTE F., BARNOLE J., FAURE C., BUTEL J., *Three-dimensional rigidity of the Ilizarov external fixator (original and modified) implanted at the femur. Experimental study and clinical deductions*, Rev. Chir. Orthop. Reparatrice Appar. Mot., 1991, 77 (2), 65–76.

[18] SILANTIEVA T.A., GORBACH E.N., *Preparing samples of biological tissues for a study using a scanning electronic microscope with camphene*, Fundamental Studies, 2015, 22 (2), 4919–4923.

[19] OOSTENBROEK H.J., BRAND R., VAN ROERMUND P.M., CASTELEIN R.M., *Paediatric lower limb deformity correction using the Ilizarov technique: a statistical analysis of factors affecting the complication rate*, J. Pediatr. Orthop. B., 2014, 23 (1), 26–31.

[20] HETTICH G., SCHIERJOTT R.A., EPPLE M., GBURECK U., HEINEMANN S., MOZAffARI-JOVEIN H., GRUPP T.M., *Calcium Phosphate Bone Graft Substitutes with High Mechanical Load Capacity and High Degree of Interconnecting Porosity*, Materials, 2019, 12, 3471.

[21] BOHNER M., BAROUD G., BERNSTEIN A., DÖBELIN N., GALEA L., HESSE B., HEUBERGER R., MEILLE S., MICHEL P., VON RECHENBERG B. et al., *Characterization and distribution of mechanically competent mineralized tissue in micropores of β-tricalcium phosphate bone substitutes*, Mater. Today, 2017, 20, 106–115.

[22] BARRERE F., VAN DER VALK C.M., DALMEIJER R.A. et al., *Osteogenecity of octacalcium phosphate coatings applied on porous metal implants*, J. Biomed. Mater Res., 2003, 66(A), 779–788.

[23] YUAN H., VAN DEN DOEL M., LI S.H. et al., *A comparison of the osteoinductive potential of two calcium phosphate ceramics implanted intramuscularly in goats*, J. Mater. Sci. Mater. Med., 2002, 13, 1271–1275.

[24] CAPLAN A., *All MSCs are pericytes*, Cell. Stem. Cell., 2008, 3(3), 229–230.

[25] SIOW R.C., MALLAWAARACHCHI C.M., WEISSBERG P.L., *Migration of adventitial myofibroblasts following vascular balloon injury: insights from in vivo gene transfer to rat carotid arteries*, Cardiovasc. Res., 2003, 59, 212–221.